Check for updates

Original Article

Anticancer Potential and Phytochemical Constituents of *Ononis natrix* Grown in Lebanon

Journal of Applied Pharmaceutical Science
16(10) 1031–1043, 2026
© The Author(s) 2026
Article reuse guidelines:
in.sagepub.com/journals-permissions-india
DOI: 10.1177/22133354261461009
journals.sagepub.com/home/phs
Sage

Aya Chouman[1], Maha Aboul Ela[1,2], Kamal Bouhadir[3], Bilal Azakir[4], Abdalla El-Lakany[1,2] and Mohamad Ali M. Hijazi[1]

Abstract

Chemotherapy faces numerous challenges, like drug resistance, severe side effects, and high costs, highlighting the need for effective and affordable alternative treatments. Natural products offer promising candidates, with Ononis species known for diverse biological activities owing to phenolic compounds. This study represents the first phytochemical and pharmacological investigation of Lebanese *Ononis natrix*. Using chromatographic techniques and spectroscopic analysis, five compounds were isolated and identified as follows: 8-hydroxy-6-methoxy-3-undecyl-3,4-dihydroisocoumarin (O1), gardenin B (O2), 5-demethylnobiletin (O3), 5-(2-hydroxytridecyl)benzene-1,3-diol (O4), and pectolinarigenin (O5). Compounds O3 and O4 are reported for the first time in Ononis species, with O4 being rare. The crude extract's (CE) and isolated compounds' anticancer activities were assessed against the human colon adenocarcinoma cell line (HT-29) and the human non-small cell lung cancer cell line (H460) using the 3-(4,5-dimethylthiazol-2-yl)-2,5-diphenyltetrazolium bromide (MTT) assay. Results revealed significant inhibitory activities of compounds O4 and O5 against both cell lines, with IC_{50} values between 21–23 µM and 32–34 µM, respectively. Interestingly, all the tested compounds and the CE showed either synergistic or additive effects when used in combination with a chemotherapeutic agent (sorafenib), achieving the same efficacy at reduced sorafenib doses (2.5 and 5 µM) and an enhanced inhibitory effect at the standard dose (10 µM). Structure-activity relationship analysis correlated O4's activity to the long side chain at C-5 and O5's to the hydroxyl and methoxy groups. These preliminary findings highlight the medicinal importance of Lebanese *O. natrix* in vitro, but no conclusion can be drawn regarding its therapeutic benefit. Further investigations are recommended to explore the remaining components and determine their biological activities and mechanisms of action.

Keywords

Ononis natrix, cytotoxicity, combination therapy, structural features, phenolic constituents, spectroscopy

Received 15 December 2025; **accepted** 24 March 2026

Introduction

Drug discovery and development is a lengthy and complex process. It consists of five main stages, starting with a pre-discovery stage, in which research on a new drug is performed, and ending with a post-market monitoring stage that determines whether the drug is approved for clinical use by the public.[1] Usually, the process takes about 10–15 years, typically costing more than $1–2 billion for a new drug to pass the final stage. In addition to these challenges, the drug

[1] Department of Pharmaceutical Sciences, Faculty of Pharmacy, Beirut Arab University, Beirut, Lebanon
[2] Department of Pharmacognosy, Faculty of Pharmacy, University of Alexandria, Egypt
[3] Faculty of Arts and Sciences, American University of Beirut, Lebanon
[4] Faculty of Medicine, Beirut Arab University, Beirut, Lebanon

Corresponding author:
Mohamad Ali M. Hijazi, Department of Pharmaceutical Sciences, Faculty of Pharmacy, Beirut Arab University, P.O. Box: 11-5020 Riad El Solh 1107 2809, Beirut, Lebanon.
E-mail: m.hijazi@bau.edu.lb

Creative Commons Non Commercial CC BY-NC: This article is distributed under the terms of the Creative Commons Attribution-NonCommercial 4.0 License (http://www.creativecommons.org/licenses/by-nc/4.0/) which permits non-Commercial use, reproduction and distribution of the work without further permission provided the original work is attributed as specified on the Sage and Open Access pages (https://us.sagepub.com/en-us/nam/open-access-at-sage).

discovery and development process faces issues like inadequate clinical efficacy and uncontrolled toxicity of drug candidates. All these factors lead to a 90% failure rate of clinical drug development.[2]

Cancer remains one of the leading causes of death worldwide, resulting in nearly 10 million deaths in 2023, with this number expected to rise substantially to 18.6 million deaths by 2050.[3] In particular, the occurrence of non-small cell lung cancer (NSCLC) and colorectal cancer (CRC) is globally increasing, making them the leading and the second leading causes of cancer death, respectively.[4,5] Unfortunately, chemotherapy, one of the cornerstones of anticancer treatment, has been proven to cause severe side effects that outweigh the benefits, limiting its use by patients.[6] Moreover, cancer cells are becoming resistant to chemotherapy and other anticancer treatments through both innate and acquired resistance mechanisms.[7] Finally, the excessive cost of chemotherapy, revealed to be $125–150/hour globally, has also restricted the use of chemotherapy.[8] All these factors, alongside the challenges faced in the drug discovery and development process, have prompted the finding of an alternative anticancer treatment that can overcome these obstacles.

Natural products, particularly medicinal plants, offer a feasible alternative to synthetic chemotherapeutic agents in the prevention and treatment of several cancer types. Not only are they a valuable source of bioactive compounds, but they are also efficient, easy, readily available in nature, and cost-effective.[9] Many examples exist for effective chemotherapeutic drugs of plant origin. Paclitaxel, which is used in the treatment of ovarian, breast, and lung cancer, was extracted from *Taxus brevifolia*.[10] Camptothecin, used for the treatment of bladder cancer, gastric cancer, and some leukemias, was also isolated from *Camptotheca acuminata*.[11] Moreover, aside from anticancer treatments, many compounds isolated from medicinal plants have been proven beneficial in the treatment of diverse diseases, such as the use of artemisinin from *Artemisia annua* in fighting malaria and silymarin from *Silybum marianum* in treating hepatic disorders.[10]

Genus Ononis, a member of the Fabaceae family (known as restharrow), is widely spread in the Atlantic Islands, West Asia, Europe, and North Africa. About 75 species have been discovered, especially near the Mediterranean Sea's coasts. The Ononis plant has recently gained scientific interest due to the presence of several active compounds displaying therapeutic benefits and cost-effectiveness. Plants of this genus have been used as anti-inflammatory, antioxidant, antitussive, diuretic, wound-healing, analgesic, antimicrobial, and anticancer agents, demonstrating their broad pharmacological profile. Many types of pharmacologically active constituents have been isolated from Ononis species, such as flavonoids, isoflavonoids, isocoumarins, resorcinol derivatives, terpenoids, and phenolic lactones.[12]

About 16 species of Ononis have been identified to grow widely in Lebanon.[13] *Ononis natrix*, also known as Yellow Restharrow, is an edible xerophytic plant that is spread throughout Africa, Southwest Europe, and the Mediterranean region, including the Levant countries. It is well-known for having therapeutic qualities like antibacterial, anti-inflammatory, diuretic, and wound-healing properties.[14] In addition, its extracts demonstrated antirheumatic, urolithiatic, and blood pressure reduction properties.[15] Phytochemical studies showed that *O. natrix* mainly contains alkylresourcinols, isocoumarins, and flavonoids.[16–19] These phenolic compounds could serve as potential remedies for fighting against cancer cells, as they have been shown to possess anticancer properties through multiple mechanisms, like inducing autophagy, apoptosis, and cell cycle arrest and inhibiting metastases and angiogenesis of cancerous cells.[20] However, to our knowledge, no reports exist on the phytochemical constituents or therapeutic potential of Lebanese *O. natrix*. Based on the reported literature, we postulated that the Lebanese *O. natrix* contains phenolic constituents possessing remarkable cytotoxic potential against cancer cells. Therefore, this study aims to investigate the phytochemical profile of the *O. natrix* plant growing in Lebanon, referred to as Lebanese *O. natrix*, and to evaluate the cytotoxic activity of the plant and/or its constituents that could be therapeutically beneficial.

Materials and Methods

Methods

Plant Material

The aerial parts of *O. natrix* were collected during the mid-flowering period of May 2023 from West Beqaa (1,300 meters above sea level). No specific permit was required for the collection of this plant species at the sampling site. Dr. George Tohme (taxonomist) from the National Council for Scientific Research, Beirut, Lebanon, authenticated the plant. A voucher sample of the plant was kept at Beirut Arab University (BAU) herbarium and given the number (ON-A2-23). Aerial parts were air-dried for 2 weeks at normal conditions and then ground to get 1.2 kg of fine powder, equivalent to approximately 4–5 kg fresh plant material, assuming 70%–80% moisture content in fresh biomass.

Preparation of Plant Extract

The air-dried powdered plant was extracted by maceration in 80% ethanol for 4–5 days successively until complete exhaustion. The extract was collected, and evaporation of the solvent was done under reduced pressure to get around 180 g of crude extract (CE).

Chromatographic Isolation of Compounds

Open-column chromatography (CC, 120 cm × 7.5 cm) was carried out on 115 g of the crude ethanol extract over silica gel (1,500 g). Elution was performed with gradient mixtures of petroleum ether and dichloromethane (PE: DCM, 22.5%–100% DCM) and then continued with dichloromethane and

methanol (DCM: MeOH, 2%–100% MeOH) to give 50 fractions (F1–F50) of 500 mL. Each fraction was analyzed by thin-layer chromatography (TLC) analysis and screened using a suitable solvent system, ultraviolet lamp detection, exposure to concentrated NH_3, and anisaldehyde/sulfuric spraying reagent. Similar fractions were combined for further purification either through CC or crystallization to get single pure crystalline compounds. Fractions F10–F14 were gathered and recrystallized into light-yellow crystals to give the compound O1. Fractions F27 and F28 were pooled again and subjected to another CC (60 × 3.2 cm) using silica gel (150 g) eluted by a gradient mixture of petroleum ether and ethyl acetate (PE: EtOAc, 33%–50% EtOAc) to give 19 fractions (F'1–F'19). Compounds O2 and O3 precipitated freely from F'3 as light-yellow crystals and from F'7 as light-yellow feather-like crystals, respectively. They were further purified by recrystallization from DCM: MeOH solution. Separation of F29–F31 (27 g) was performed using CC (85 cm × 4.5 cm) over silica gel (340 g) and eluted with gradient mixtures of petroleum ether and ethyl acetate (PE: EtOAc, 25%–50% EtOAc) to give 20 fractions (F''1–F''20), where compound O4 was obtained after recrystallization of F''7 from the DCM: MeOH solution and compound O5 was obtained after recrystallization of F''18 from the DCM: MeOH solution as yellow needles.

Anticancer Screening

The anti-tumor activity of the CE and isolated compounds was examined against two cancer cell lines: the human colorectal cell line (HT-29) and the human lung cell line (H460). The HT-29 cell line was cultured in Roswell Park Memorial Institute (RPMI) 1,640 medium, whereas H460 was cultured in Dulbecco's Modified Eagle Medium (DMEM). 10% fetal bovine serum (FBS), 2 µM L-glutamine, and 1% penicillin/streptomycin were added to both media. The cells were incubated at 37°C in a humidified environment with 5% CO_2. For 3-(4,5-dimethylthiazol-2-yl)-2,5-diphenyltetrazolium bromide (MTT), a 96-well plate was seeded with 7×10^3 cells per well in the appropriate culture media, and the plate was incubated for 24 hours at 37°C with 5% CO_2. After that, stock solutions (1 mg/mL) from the CE and (1 M) from each of the compounds were freshly prepared by dissolving the samples in a dimethyl sulfoxide (DMSO) solution. Working solutions with different concentrations (10, 25, 50, 75, 100 and 200 µg/mL) for CE and (10, 25, 50, 75, 100 and 200 µM) for all the other compounds were then prepared from the stock solutions. After 24 h, the cells were treated with 100 µL of these different concentrations of CE and compounds for 72 h. Only cells in their appropriate media were present in the control wells, whereas cells in media containing 0.2% DMSO were present in the mock wells. The concentration range 10 to 200 µM was based on preliminary experiments to test the dose range responses.

Cell viability was evaluated using an MTT assay: 50 µL of a 5 mg/mL MTT solution was added to the wells after the medium was removed. The blank comprised media with 10% MTT and no cells. After 4 h of incubation, 50 µL of DMSO was added to the wells, and plates were shaken gently for 2 min to dissolve the formed formazan crystals. The absorbance was measured at 620 nm using an ELISA reader (Thermo Fisher Scientific, Boston, MA, USA). The experiment was repeated in triplicate. Results were reported in terms of % cell viability ± SD using the following equation: % *Cell viability* = $[(At - Ab)/Am] \times 100$, where *At* is the absorbance of the tested sample, *Ab* is the blank absorbance, and *Am* is the absorbance of the mock. Drugs were added as indicated. Sorafenib was added in the absence or presence of the indicated concentration of drugs.

The IC_{50} (the concentration that reduced cell viability to 50%) was determined for each variety against each cell line using MicroCell Origin software by non-linear regression analysis using the dose–response equation. IC_{50} was used to compare the cytotoxic activities of the tested extract and compounds.

The dual effect of sorafenib and each of the compounds or the CE was determined using the modified Burgi formula (i.e., the Jin equation).[21,22] The formula is $q = EA + EB/ (EA + EB - EA \times EB)$, where EA + B, EA, and EB are the average effects of the combination treatment, CE, or compounds alone, and sorafenib alone, respectively. As an example, if compound A produces 40% inhibition (EA = 0.40), sorafenib produces 30% inhibition (EB = 0.30), and the combination produces 60% inhibition (EA+B = 0.60), the q value is calculated as: $q = 0.60/(0.40 + 0.30 - 0.40 \times 0.30)$. Following the proposed Jin et al. criteria, antagonism is when $q < 0.85$, an additive effect if $0.85 \leq q \leq 1.15$, and a synergistic effect if $q > 1.15$.

Sorafenib stock solutions were dissolved in DMSO, followed by a dilution in the corresponding cell medium to obtain a final concentration of either 2.5, 5, or 10 µM. For the combination condition, all cells were simultaneously treated with both sorafenib and either the CE or isolated compounds at the studied concentrations. Control treatments were either sorafenib alone, extract/compound alone, or vehicle control. The tested concentration included a sub-lethal dose to assess the dose-dependent effects and to accurately determine the IC_{50}.

Statistical Analysis

All these experiments were performed at least in triplicate, and data are presented as mean ± standard deviation (SD). Differences between control and treatment doses were assessed using the Student's *t*-test. Significance level was set at $p < .05$.

Materials and Reagents

Solvents

All organic solvents for CC and TLC (PE, DCM, MeOH, and EtOAc), DMSO-d_6 for nuclear magnetic resonance (NMR), and DMSO for MTT were obtained from Sigma–Aldrich

(Germany, analytical grade). PE, DCM, MeOH, and EtOAc used for recrystallization and analysis were HPLC-grade from Sigma–Aldrich.

Chemicals

Silica gel for CC (technical grade, pore size 60 A, 70–230 mesh, 63–200 μm) was purchased from Sigma–Aldrich (Germany); silica gel for CC 60–200 mesh (74–250 μm) was purchased from Himedia (India); and TLC plates (silica gel 60 F_{254}) were purchased from Macherey-Nagel (Germany).

Apparatus

Spectrophotometer

Bruker Alpha FT-IR Spectrometer, wavelength range (400–4,000 cm^{-1}), spectral resolution: 2 cm^{-1}, dimensions (W × D × H): 220 × 330 × 260 mm.

NMR Spectrometer

All NMR data of the examined samples were measured on a Bruker Ascend™ 500 spectrometer fitted with Advance III HD, using deuterated solvents $CDCl_3$, CD_3OD, and DMSO-d_6.

Cancer Cell Lines

HT-29 and H460 cancer cell lines were obtained from Dr. Marwan Sabban (American University of Beirut) and Dr. Salem Chouaib (Gulf Medical University), respectively. Both cell lines were originally purchased from ATCC, and short tandem repeat (STR) profiling was not performed by our laboratory upon reception. All experiments were conducted at low passage numbers (8–12 passages) to reduce the phenotypic drift. All cells were tested for mycoplasma after thawing using a PCR-based mycoplasma detection kit and DAPI staining.

Results and Discussion

Phytochemical Investigation of *O. natrix*

Full spectroscopic analysis was done for the isolated compounds, including NMR (^{1}H-NMR, ^{13}C-NMR, DEPT-135, HMBC, HSQC, NOESY, COSY) and FT-IR (see Supplementary Materials, Figures S1–S35). The spectroscopic data are summarized in Tables 1 and 2 for the ^{1}H-NMR and ^{13}C-NMR data of isolated compounds.

Structural Elucidation

This study represents the first phytochemical investigation of Lebanese *O. natrix*, contributing to the limited evidence on the chemical composition of the Lebanese species of this plant.

Five compounds were isolated and identified as8-hydroxy-6-methoxy-3-undecyl-3,4-dihydroisocoumarin (O1), gardenin B (O2), 5-demethylnobiletin (O3), 5-(2-hydroxytridecyl)benzene-1,3-diol (O4), and pectolinarigenin

Table 1. ^{1}H-NMR Data for Isolated Compounds from *O. natrix* (at 500 MHz, ppm, *J* in Hz).

H	O1 ($CDCl_3$)	O2 (DMSO-d_6)	O3 ($CDCl_3$)	O4 (CD_3OD)	O5 (DMSO-d_6)
2	–	–	–	6.09 (1H, t, *J* = 2)	–
3	4.52 (1H, m)	6.54 (1H, s)	6.64 (1H, s)	–	6.87 (1H, s)
4	2.87 (2H, m)	–	–	6.14 (1H, d, *J* = 2)	–
5	6.26 (1H, d, *J* = 2)	–	–	–	–
6	–	–	–	6.14 (1H, d, *J* = 2)	–
7	6.37 (1H, d, *J* = 2)	–	–	–	–
8	–	–	–	–	6.61 (1H, s)
1'	1.74 (20H, m)	–	–	2.46 (H_a-1', dd, *J* = 15, 7.5) 2.44 (H_b-1', dd, *J* = 15, 7.5)	–
2'	1.74 (20H, m)	7.83 (1H, d, *J* = 9)	7.44 (1H, d, *J* = 2)	3.32 (1H, m)	8.03 (1H, d, *J* = 9)
3'	1.74 (20H, m)	6.97 (1H, d, *J* = 9)	–	1.57 (2H, m)	7.10 (1H, d, *J* = 9)
4'	1.74 (20H, m)	–	–	1.30 (18H, m)	–
5'	1.74 (20H, m)	6.97 (1H, d, *J* = 9)	7.02 (1H, d, *J* = 8.5)	1.30 (18H, m)	7.10 (1H, d, *J* = 9)
6'	1.74 (20H, m)	7.83 (1H, d, *J* = 9)	7.61 (1H, dd, *J* = 2, 8.5)	1.30 (18H, m)	8.03 (1H, d, *J* = 9)
7'	1.74 (20H, m)	–	–	1.30 (18H, m)	–
8'	1.74 (20H, m)	–	–	1.30 (18H, m)	–
9'	1.74 (20H, m)	–	–	1.30 (18H, m)	–
10'	1.74 (20H, m)	–	–	1.30 (18H, m)	–
11'	0.89 (3H, t, *J* = 7)	–	–	1.30 (18H, m)	–
12'	–	–	–	1.30 (18H, m)	–
13'	–	–	–	0.91 (3H, t, *J* = 6)	–

(Table 1 continued)

(Table 1 continued)

H	O1 ($CDCl_3$)	O2 (DMSO-d_6)	O3 ($CDCl_3$)	O4 (CD_3OD)	O5 (DMSO-d_6)
5-OH	–	12.74 (1H, s)	12.56 (1H, s)	–	13.04 (1H, s)
6-OCH_3	3.83 (3H, s)	3.88 (3H, s)	3.97 (3H, s)	–	3.75 (3H, s)
7-OH	–	–	–	–	10.77 (1H, s)
7-OCH_3	–	4.04 (3H, s)	3.99 (3H, s)	–	–
8-OH	11.27 (1H, s)	–	–	–	–
8-OCH_3	–	3.91 (3H, s)	4.003 (3H, s)	–	–
3'OCH_3	–	–	4.009 (3H, s)	–	–
4'OCH_3	–	3.81 (3H, s)	4.13 (3H, s)	–	3.85 (3H, s)

Table 2. ^{13}C-NMR Data for Isolated Compounds from *O. natrix* (at 126 MHz, in ppm, *J* in Hz).

C	O1 ($CDCl_3$)	O2 ($CDCl_3$)	O3 ($CDCl_3$)	O4 (DMSO-d_6)	O5 (DMSO-d_6)
1	169.95 (C)	–	–	158.61 (C)	–
2	–	164.13 (C)	163.94 (C)	100.38 (C)	163.81 (C)
3	79.21 (C)	103.71 (C)	104 (C)	158.61 (C)	103.50 (C)
4	33.16 (C)	183.05 (C)	183 (C)	106.72(C)	182.64 (C)
5	106.17 (C)	149.5 (C)	149.55 (C)	144.66(C)	153.12 (C)
6	165.72 (C)	136.51 (C)	136.56 (C)	106.38 (C)	131.82 (C)
7	99.37 (C)	152.98 (C)	152.44 (C)	–	157.80 (C)
8	164.48(C)	132.98 (C)	132.93 (C)	–	94.77 (C)
9	101.76 (C)	145.81 (C)	145.8 (C)	–	152.90 (C)
10	141.09 (C)	106.96 (C)	106.99 (C)	–	104.59 (C)
1'	34.78 (C)	123.41 (C)	123.66 (C)	35.77(C)	123.29 (C)
2'	24.86 (C)	128.12 (C)	108.66 (C)	49.05 (C)	128.66 (C)
3'	29.36 (C)	114.62 (C)	149.34 (C)	31.79 (C)	115.03 (C)
4'	29.38(C)	162.78 (C)	153.02 (C)	31.23(C)	162.76 (C)
5'	29.49 (C)	114.62 (C)	111.23 (C)	29.54 (C)	115.03 (C)
6'	29.57(C)	128.12 (C)	120.17 (C)	29.51 (C)	128.66 (C)
7'	29.63(C)	–	–	29.41(C)	–
8'	29.65(C)	–	–	29.21 (C)	–
9'	31.93 (C)	–	–	29.19 (C)	–
10'	22.71 (C)	–	–	29.13 (C)	–
11'	14.28 (C)	–	–	29.01 (C)	–
12'	–	–	–	22.38 (C)	–
13'	–	–	–	13.10 (C)	–
6-OCH_3	55.55 (C)	61.17 (C)	61.19 (C)	–	60.32 (C)
7-OCH_3	–	61.75 (C)	62.12 (C)	–	–
8-OCH_3	–	62.19 (C)	61.78 (C)	–	–
3-OCH_3	–	–	56.01 (C)	–	–
4-OCH_3	–	55.58 (C)	56.16 (C)	–	56.02 (C)

(O5) using extensive spectroscopic analysis. Interestingly, O3 is a compound that is characteristic of the genus Citrus[23] and has not been isolated from the genus Ononis before. Additionally, O4 is a rare compound that has only been reported twice before and never in Ononis species. The identification of these unique compounds highlights the potential of Lebanese *O. natrix* as a source of structurally diverse and bioactive secondary metabolites and emphasizes the importance of exploring endemic flora, particularly in regions like Lebanon, where biodiversity remains underexplored. The chemical structures of the isolated compounds are summarized below in Figure 1.

FT-IR spectra of compounds O2, O3, and O5 showed the presence of aromatic rings A and B (absorption bands at ~1,460 cm^{-1}, ~1,570 cm^{-1}) and a carbonyl group stretching in benzopyrone ring C (absorption band at ~1,655 cm^{-1}). ^{1}H-NMR and ^{13}C-NMR spectra were consistent with a flavone skeleton. A characteristic signal in the ^{13}C-NMR at

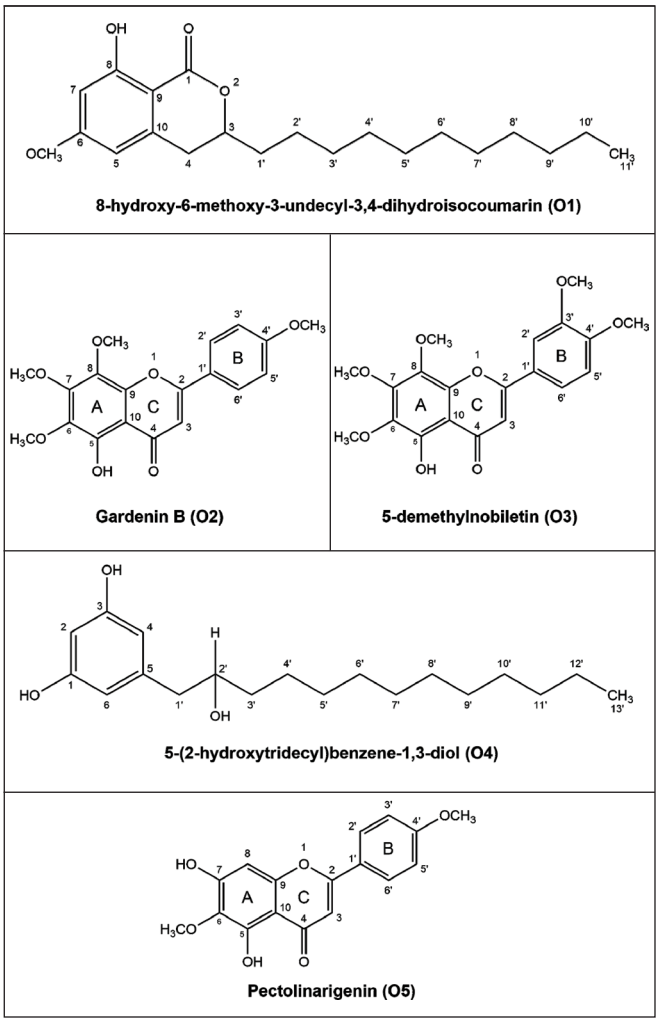

Figure 1. Chemical Structures of Compounds O1–O5.

the downfield region δ 165–180 was evident for a carbonyl group at C-4, and signals at δ 164–166, and δ 104–110 indicated the presence of a C2-C3 double bond conjugated to the carbonyl. In the ^{1}H-NMR spectra, a singlet aromatic proton signal appeared at δ 6.5–6.9 (1H, s) and was linked to C-3, typical for flavones. Moreover, a singlet proton signal at δ 12–14 (1H, s) indicated the presence of a phenolic hydroxyl group located at C-5 in these compounds.

O2 was obtained as light-yellow crystals. ^{13}C-NMR and DEPT-135 spectra showed seventeen carbon signals classified as four methyl, three methines, and 10 quaternary carbons. The observed ^{13}C-NMR signals were fewer than the total number of carbons in the molecular formula due to structural symmetry. Two pairs of equivalent methine carbons were present, showing signals at δ 128.12 and δ 114.62. The presence of two doublet aromatic proton signals in the ^{1}H-NMR at δ 7.83 and 6.97 (each 1H, d, J = 9 Hz) was correlated with the ^{13}C-signals at δ 128.12 and 114.62, respectively. Moreover, the presence of four methine groups located at C2', C3', C5', and C6' was confirmed by HSQC and HMBC experiments. Furthermore, the ^{1}H-NMR spectrum indicated the presence of four methoxy groups at δ 3.88, 4.04, 3.91, and 3.81 (each 3H, s) correlated to carbons C-6 (δ 61.17), C-7 (δ 61.75), C-8 (δ 62.19), and C-4' (δ 55.58), respectively, based on reported literature.[23] Accordingly, compound O2 is the tetra-methoxylated flavone, 5-demethyltangeretin, known as gardenin B, and has the molecular formula ($C_{19}H_{18}O_7$). All these assignments were in good agreement with the data available in the literature.[23]

O3 was isolated in the form of light-yellow, feather-like crystals. ^{13}C-NMR and DEPT-135 spectra showed twenty carbon signals: five methyl, four methines, and eleven quaternary carbons. The ^{1}H-NMR and ^{13}C-NMR spectra are remarkably similar to those of compound 2. The difference lies at C3', where instead of having an aromatic proton like O2, there is a methoxy group present that appeared as an additional singlet signal at δ 4.009. All this data suggested that compound O3 is the penta-methoxylated flavone, 5-demethylnobiletin, with the molecular formula ($C_{20}H_{20}O_8$). All these assignments were in good agreement with the data available in the literature.[23,24]

Finally, O5 was isolated in the form of yellow, needle-shaped crystals. ^{13}C-NMR spectra showed fifteen carbon signals: two methyl, four methines, two of which have a strong peak, meaning the presence of two more methine groups, and nine quaternary carbons. The observed ^{13}C-NMR signals were fewer than the total number of carbons in the molecular formula due to structural symmetry. Two pairs of equivalent methine carbons were present, showing signals at δ 115.03 and δ 128.66. The ^{1}H-NMR of O5 is also like that of O3, but the difference lies at C-7 and C-8, where a singlet proton signal appearing at δ 10.77 signifies the presence of a phenolic hydroxy group located at C-7. An additional aromatic proton signal was also observed at δ 6.61 (1H, s) and was assigned to C-8. All this data suggested compound O5's structure to be the dimethoxylated flavone, pectolinarigenin, having the molecular formula ($C_{17}H_{14}O_6$). All these assignments were in good agreement with the data available in the literature.[25]

Full structural elucidation of compounds O2, O3, and O5 was confirmed from a combined analysis of FT-IR, ^{1}H and ^{13}C-NMR, DEPT-135, HSQC, and HMBC spectra (Tables 1 and 2).

Compounds O1 and O4 also share some similarities in their structures, as ^{13}C-NMR and ^{1}H-NMR spectra of both compounds revealed skeletons of alkylated aromatic systems. ^{1}H-NMR signals appeared at δ 1.2–1.4, signaling the presence of an undecane chain in O1 at C-3 and a tridecane chain in O4 at C-5, with terminal methyl groups at $\delta \sim$ 0.9 (3H, t) in both compounds.

Compound O1 was isolated in the form of light-yellow crystals. The presence of a small absorption band at ~1,740 cm^{-1} and a sharp band at ~1650 cm^{-1}, as well as two bands at ~1,583 cm^{-1} and ~1,480 cm^{-1} in the FT-IR spectrum demonstrates the presence of a six-membered lactone ring fused to a benzene ring. ^{13}C-NMR and DEPT-135 spectra showed

21 carbon signals: two methyl, eleven methylene, three methines, and five quaternary carbons. ^{1}H-NMR spectrum showed a signal (δ 11.27, 1H, s) indicating the presence of a phenolic hydroxyl group adjacent to the carbonyl group. The two aromatic protons (δ 6.26 and 6.37, d, J = 2 Hz) in the *meta* position appeared as doublets and were assigned to C-5 (δ 106.17) and C-7 (δ 99.37), respectively. HMBC correlations showed that the benzylic methylene (δ 2.87, 2H, m) located at C-4 (δ 33.16) is coupled with the proton (δ 4.52, m) of a methine group bearing an oxygenated group (δ 79.21) and is slightly coupled with the aromatic proton at δ 6.26. In addition, an aromatic methoxy group (δ 3.83, 3H, s) was assigned to C-6 (δ 165.72) based on HSQC and HMBC correlations and its coupling to the aromatic protons at δ 6.261 and 6.374. The molecular formula ($C_{21}H_{32}O_4$) was derived from a combined analysis of FT-IR, ^{1}H and ^{13}C-NMR spectra (Tables 1 and 2). Based on these interpretations, O1 is a dihydroisocoumarin, and its structure was confirmed to be 8-hydroxy-6-methoxy-3-undecyl-3,4-dihydroisocoumarin. All these assignments were in good agreement with data available in the literature.[17,26]

Compound O4 was obtained in the form of friable red crystals. The presence of an alcoholic hydroxyl group was designated by an absorption band at ~3,440 cm^{-1} in the FT-IR spectrum. ^{13}C-NMR and DEPT-135 spectra showed 19 carbon signals classified as one methyl, eleven methylene, four methines, and three quaternary carbons. Two proton signals in the aromatic region appeared in the ^{1}H-NMR. The first signal, which showed up as a triplet at δ 6.09 (1H, t, J = 2 Hz), indicated the presence of an aromatic proton at position C-2 (δ 100.38). The second signal appeared as a doublet at δ 6.14 (1H, d, J = 2 Hz) and was located at C-4 and C-6 (δ 106.38). Moreover, the positions of the two equivalent aromatic hydroxyl groups at positions 1 and 3 were assigned based on HMBC correlations. Additionally, a signal of a benzylic methylene group (δ 2.44, 2H, dd, J = 15 Hz, 7.5 Hz) appeared at C-5 (δ 144.66). The proton signal δ 3.32 (1H, m) suggests the presence of a hydroxy group at position C-2'. High-resolution mass spectroscopy HRMS (ESI^{+}) showed a protonated molecular ion at m/z 309.2424 corresponding to $[M+H]^{+}$ for this compound to confirm the molecular formula ($C_{19}H_{32}O_3$). The combined analysis of ESI^{+} MS at m/z 309.2424 $[M+H]^{+}$, FT-IR, ^{1}H and ^{13}C-NMR, DEPT-135, HSQC, HMBC, COSY, and NOESY spectra (Tables 1 and 2) leads to the confirmation of the structure of compound O4 as 5-(2-Hydroxytridecyl)benzene-1,3-diol, which is an alkyl resorcinol that appears to be a rare compound not separated or identified in Ononis species before.

Anticancer Activity of O. natrix and Isolated Compounds

The anticancer activities of *O. natrix* CE and compounds O1, O4, and O5 have not been assessed against HT-29 and H460 cancer cell lines before, so our study represents the first report to evaluate their anticancer activities against these cell lines. The anticancer activity of *O. natrix* CE and isolated compounds was evaluated through their inhibitory effect against HT-29 and H460 cancer cell lines. The figures below show the inhibitory effect of the CE and the five isolated compounds on the two cancer cell lines (H460 and HT-29) alone, using different doses. Results showed a dose-dependent inhibitory activity of the CE and isolated compounds, with compounds O4 and O5 having the highest activities (Figures 2 and 3).

HT-29 is a human colorectal adenocarcinoma cell line which is commonly used as a CRC in vitro model. H460 is

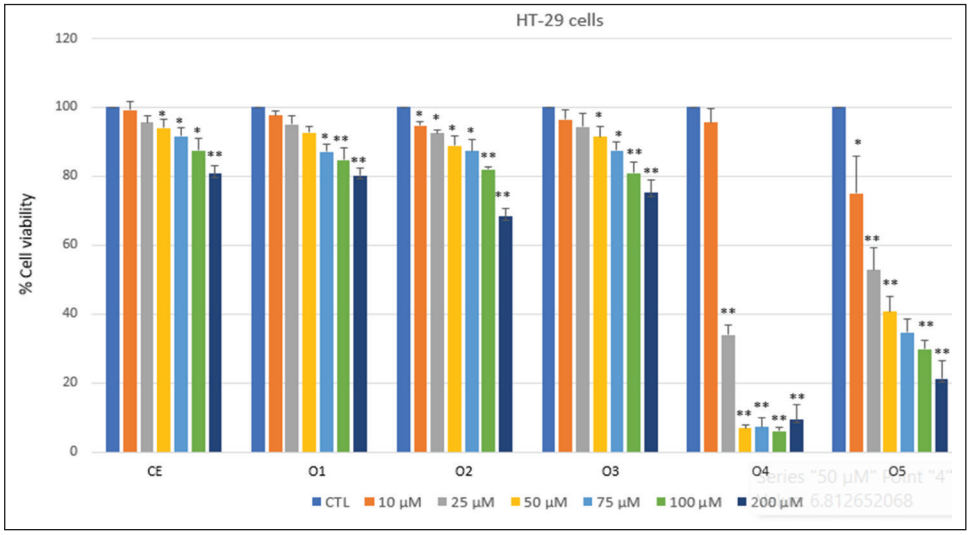

Figure 2. The Anti-tumor Activity of *O. natrix* Extract and Isolated Compounds on HT-29 Cells at Different Concentrations.

Notes: Represented data are the average of three different determinations ± SD.
Only for CE, the concentrations are represented as (µg/mL).

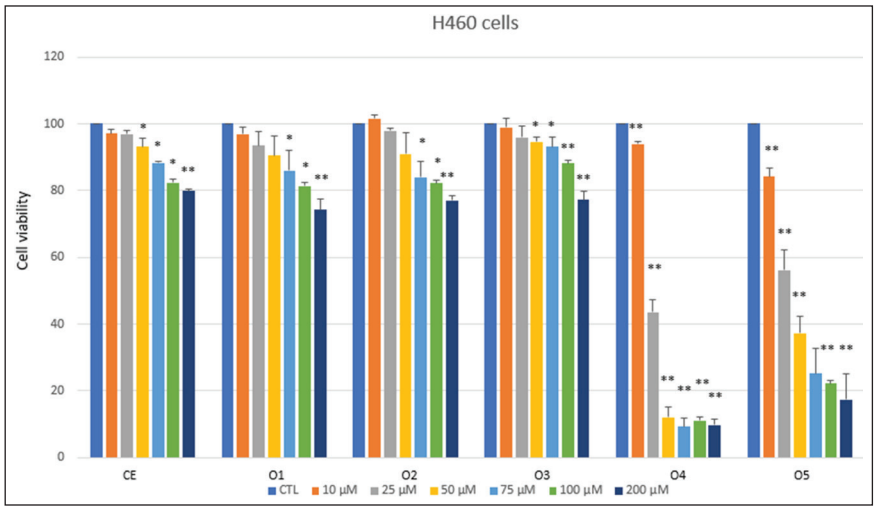

Figure 3. The Anti-tumor Activity of *O. natrix* Extract and Isolated Compounds on H460 Cells at Different Concentrations.

Notes: Represented data are the average of three different determinations ± SD.
* and ** means *p* value <.05 and *p* value <.01, respectively.
Only for CE, the concentrations are represented as (µg/mL)

a human NSCLC cell line harboring a KRAS mutation yet retaining wild-type p53 status.[27,28] Therefore, these two cell lines are adequate to conduct a preliminary evaluation of the cytotoxic activity of the samples in both lung and CRC models.

The IC_{50}, which is the minimum concentration of the drug required to kill or inhibit 50% of tumor cells, was calculated for the CE and isolated compounds (Table 3). Results revealed weak inhibitory activities of CE and compounds O1, O2, and O3 against both H460 and HT-29 cell lines, with IC_{50} more than 200 µM (or 200 µg/mL for CE). On the other hand, significant inhibitory activities were obtained by compounds O4 and O5 against both tested cell lines, with IC_{50} values between 21 and 23 µM and 32 and 34 µM, respectively. It was noticed that the IC_{50} values for both compounds (O4 & O5) do not vary significantly between the two cell lines, suggesting a similar mechanistic pathway that needs to be further investigated. In contrast to our results, the methanolic extract of Jordanian *O. natrix* was effective against prostate cancer cells PC-3 (IC_{50} = 55 ± 2 µg/mL) and liver cancer cells HepG-2 (IC_{50} = 68 ± 2 µg/mL) when compared to cisplatin (positive control). The extract also showed anticancer activity against CaCo-2 colon adenocarcinoma (IC_{50} = 109 ± 2 µg/mL), MCF-7 breast cancer (IC_{50} = 123 ± 2 µg/mL), and HeLa immortalized (IC_{50} = 79 ± 1 µg/mL) cell lines.[29] Additionally, the anticancer activity of compounds O2 and O3 was evaluated against the HT-29 cell line using 5-fluorouracil as a positive control (IC_{50} = 42.12 µg/mL). IC_{50} values of 62.35 and 132.14 µg/mL were obtained, respectively, indicating a high anticancer activity for O2 against this cell line.[30] O2 was also shown to have a strong antiproliferative activity against breast, hepatic, lung, colon, and leukemia cell lines and keratinocytes (IC_{50} 12.82 ± 0.67–94.63 ± 1.27 µg/mL).[31] The cytotoxic effects of the studied samples are presented as dose–response curves (Figures 2 and 3), while the calculated IC_{50} values are summarized in Table 3. These discrepancies could be attributed to differences in experimental conditions, mainly the cancer cell lines used: HT-29 and H460 in the present study compared to PC-3, HepG-2, CaCo-2, MCF-7, and HeLa in the previous studies. Differences in assay parameters and concentration ranges tested can also cause such discrepancies. In addition, variations in compound purity, stability, or potential synergistic interactions with other phytochemicals in the plant extract may also influence the observed biological activity.

Table 3. IC_{50} of the CE and Isolated Compounds O1–O5 Against H460 and HT-29 Cancer Cell Lines.

	Average of IC_{50}	
Sample	H460	HT-29
CE (in µg/mL)	>200	>200
O1 (in µM)	>200	>200
O2 (in µM)	>200	>200
O3 (in µM)	>200	>200
O4 (in µM)	23.694	21.025
O5 (in µM)	34.390	32.860

To evaluate the potential of the Ononis plant and its pure compounds in cancer therapy, the effect of sorafenib in combination with the pure compounds (in concentrations of 100 or 200 µM) or the CE (in concentrations of 100 or 200 µg/mL) was studied against both cancer cells (Table 4, see Supplementary Materials, Figures S36–S37). Sorafenib, an FDA-approved drug, is an oral multitargeted tyrosine kinase inhibitor that is used in the treatment of hepatocellular, renal cell, and thyroid cancers.[32] According to the label issued by the FDA, sorafenib has many adverse effects, including

Table 4. Interaction Effect of the Tested Samples with 5 µM Sorafenib Based on Inhibition % Using the Jin/Burgi Equation, Where *q* Value <0.85: Antagonist, *q* Value Between 0.85 and 1.15: Additive, and *q* Value >1.15: Synergistic.

		Viability %		Inhibition %		Combination Index Score	
Sample		HT-29	H460	HT-29	H460	HT-29	H460
Sorafenib	5 µM	60.76	75.46	39.24	24.54	–	–
CE	100 µg/mL – Soraf	96.55	94.68	3.45	5.32	1.26	1.2
	100 µg/mL + Soraf	47.81	64.02	52.19	35.98	(Synergistic)	(Synergistic)
	200 µg/mL –Soraf	66.46	85.4	33.54	14.6	1.21	1.4
	200 µg/mL + Soraf	27.32	50.06	72.68	49.94	(Synergistic)	(Synergistic)
O1	100 µM –Soraf	64.95	81.72	35.05	18.28	1.11	1.54
	100 µM + Soraf	32.46	40.77	67.54	59.23	(Additive)	(Synergistic)
	200 µM –Soraf	33.13	69.94	66.87	30.06	0.88	1.28
	200 µM + Soraf	29.26	39.27	70.74	60.73	(Additive)	(Synergistic)
O2	100 µM –Soraf	49.59	69.83	50.41	30.17	1	1.03
	100 µM + Soraf	29.46	50.94	70.54	49.06	(Additive)	(Additive)
	200 µM –Soraf	30.5	60.06	69.5	39.94	0.93	0.95
	200 µM + Soraf	23.62	47.58	76.38	52.42	(Additive)	(Additive)
O3	100 µM –Soraf	52.22	65.7	47.78	34.3	1.03	0.99
	100 µM + Soraf	29.6	49.6	70.4	50.4	(Additive)	(Additive)
	200 µM –Soraf	38.48	50.14	61.52	49.86	1.04	0.98
	200 µM + Soraf	19.8	38.8	80.2	61.2	(Additive)	(Additive)
O4	IC_{50} – Soraf	47.28	32.41	52.72	67.59	1.19	1.11
	IC_{50} + Soraf	14.7	15.76	85.3	84.24	(Synergistic)	(Additive)
O5	IC_{50} – Soraf	53.05	48.68	46.95	51.32	0.95	0.91
	IC_{50} + Soraf	35.4	42.14	64.6	57.86	(Additive)	(Additive)

The single-agent values presented in this table were obtained as part of the combination experiments and represent experimental runs independent of those used for IC_{50} determination in Table 3. Combination effects were classified according to the Jin equation as synergistic, additive, or antagonistic.

cardiovascular events, hypertension, bleeding, dermatologic toxicities, QT prolongation, gastrointestinal perforation, embryo-fetal toxicity, and drug-induced liver injury.[33]

Results revealed that despite the high IC_{50} of the CE on HT-29 and H460 cancer cells, it exhibited a synergistic activity when used in combination with sorafenib (q value > 1.15 against both cell lines). Similarly, the inhibition of compounds O1, O2, and O3 was low alone yet showed either additive or synergistic effects against both cell lines. Moreover, the active compounds O4 and O5 display synergistic and additive effects against HT-29 and H460 cells, respectively, for O4 and an additive effect for O5. Some studies aimed to examine the mechanistic pathways explaining the behavior of these compounds in combination. Compound O2 was able to cause cell death in human leukemia cells and was the most cytotoxic compound against HL-60 leukemia and U-937 lymphoma cells with IC_{50} values between 1.6 and 3.0 µM.[34] Regarding compound O3, it significantly inhibits leukemia cell proliferation in acute myeloid leukemia,[35] increases apoptosis, and suppresses tumor growth in lung cancer cell lines when used in combination with the highly effective chemotherapeutic drug, paclitaxel,[36] so this could explain its additive effect. O3 has also demonstrated a cytotoxic effect on HT-29 cells, mostly by cell cycle arrest and apoptosis induction, with an IC_{50} of 8.5 µM,[37] as well as by decreasing proliferation, CDK2, and pRb, and increasing p21 and Rb expressions, with an IC_{50} of 22 µM.[38] Additionally, O5 was shown to activate autophagy, inhibit cell migration and invasion, target ERK1/2 MAP kinases, and arrest the cell cycle at the G2/M phase in cisplatin-resistant hepatocellular carcinoma.[39] Moreover, O5's activity against bladder cancer was proven to inhibit late autophagic flux and worked as a good DNA topoisomerase II alpha (TOP2A) poison.[40] Its activity against breast cancer was also studied, and revealed that it was able to cause apoptosis, inhibit tumor cell self-renewal, and downregulate Bcl2 expression, fully inhibiting it at the dose of 25 µM.[41]

These findings suggest the potential benefits of Ononis plant extract and its pure compounds as a candidate supportive compound for combination anticancer strategies in lung or colon cancers to potentiate the effect of chemotherapeutic agents, reduce the resistance of cancer cells, and enhance the in vitro effect of sorafenib. Although Ononis has been reported as an edible plant,[14] further mechanistic, toxicity, pharmacokinetic, and in vivo studies are required before any clinical relevance can be inferred. This suggestion is supported by previous research demonstrating how specific compounds can potentiate the cytotoxic effects of chemotherapeutic agents. For instance, significant antioxidant and anti-tumor benefits, as well as enhanced morphology of the induced liver damage, were seen by the combined quercetin/sorafenib treatment in hepatocellular carcinoma. The benefit of the combination intervention's efficacy can be ascribed to quercetin's notable modulation of inflammation, oxidative stress, apoptosis, and cell cycle arrest.[42]

To further explore the potential effect of these compounds as experimental adjuvants in combination with

Table 5. Viability and Inhibition (in %) of H460 and HT-29 Cells Against Different Concentrations of CE and Isolated Compounds in Combination with Sorafenib, Where Inhibition % = 100% − Viability %.

	Viability %		Inhibition %	
Sample	H460	HT-29	H460	HT-29
Soraf 10 µM	43.11	28.68	56.89	71.32
CE 200 µg/mL + Soraf 5 µM	44.92	27.48	55.08	72.52
CE 200 µg/mL + Soraf 10 µM	24.81	12.4	75.19	87.6
O1 100 µM + Soraf 5 µM	41.69	28.96	58.31	71.04
O1 200 µM + Soraf 5 µM	36.07	25.45	63.93	74.55
O1 100 µM + Soraf 10 µM	23.11	13.2	76.89	86.8
O2 200 µM + Soraf 2.5 µM	42.87	27.9	57.13	72.1
O2 100 µM + Soraf 10 µM	27.37	10.67	72.63	89.33
O3 100 µM + Soraf 5 µM	43.77	29.8	56.23	70.2
O3 100 µM + Soraf 10 µM	24.4	16.56	75.6	83.44
O4 IC_{50} + Soraf 10 µM	29.58	28.26	70.42	71.74
O5 IC_{50} + Soraf 10 µM	26	25.88	74	74.12

other anticancer therapies, we evaluated the effects of the CE and each of the compounds with the standard dose of sorafenib, 10 µM, and with lower doses, 2.5 and 5 µM (Table 5, see Supplementary Materials, Figures S38–S43). The inhibition percentages of sorafenib at 10 µM were 57% and 70% against H460 and HT-29 cells, respectively. Surprisingly, these inhibitions were comparable with 5 µM of sorafenib when combined with 200 µg/mL of CE,100 µM of O1 or O3. Moreover, the combination of 200 µM of O2 with 2.5 µM sorafenib resulted in the same inhibition percentages as 10 µM sorafenib alone. More than that, the addition of 200 µg/mL of CE or 100 µM of compounds O1, O2, or O3 markedly increased the inhibition activity of 10 µM sorafenib from 57% to more than 72% against H460 and from 70% to more than 83% against HT-29. Similarly, the combination of 10 µM of sorafenib with the IC_{50} of O4 and O5 resulted in higher inhibition percentages (~70% for O4 and ~74% for O5 against both cell lines) than sorafenib alone. While no studies have specifically reported the efficacy of natural compounds in combination with reduced doses of sorafenib, existing literature highlights their role as adjuvant therapies in decreasing sorafenib-induced side effects, particularly its cardiotoxic effects. For example, sorafenib-induced cardiotoxicity was reduced through the inhibition of the TLR4/NLRP3 signaling pathway when the flavanone hesperetin was used in combination with sorafenib. In addition, N-acetylcysteine, a natural antioxidant, may decrease sorafenib-induced apoptosis by protecting myocytes.[43]

Structure-activity Relationship in Anticancer

Studies revealed that methoxy substitution on ring A is the pharmacophore of the anticancer activity in methoxyflavones, with C-3' and C-4' on ring B reinforcing this effect. The methoxy group added lipophilicity to the flavones, causing a significant anticancer activity against different cell lines. Alternatively, a hydroxyl group is needed to maintain a strong anticancer activity in these compounds. In general, the presence of methoxy groups on at least two out of three positions from C-6, 7, and 8 positions yields a strong IC_{50}, with C7-OCH_3 substitution having a strong cytotoxic activity. Similarly, C7-OH and at least one C6-OCH_3 group exhibited the same effect. Additionally, a C5-OH group showed a strong anticancer effect, attributed to the formation of intramolecular hydrogen bonding with the C-4 carbonyl group. However, despite the importance of methoxy groups on ring B in having a strong activity, excessive substitution greatly declined the IC_{50} on various cell lines.[44] Looking at our results, O2 and O3, being tetra and pentamethoxylated, respectively, and hydroxylated at C-5, showed weak anticancer activities, opposed to the available literature on structure-activity relationship. This discrepancy could be attributed to the same reasons mentioned above, as well as to the context-dependent nature of SAR observations. Regardless, it remains a limitation worthy of further investigation. On the other hand, O5, which is dimethoxylated at C-6 and C-4' and dihydroxylated at C-5 and C-7, exerted a strong anticancer activity, aligning well with established findings. As for alkyl resorcinols, their cytotoxicity is significantly influenced by the side chain length and unsaturation. Particularly, hydrophobic substitutions at C-5 and shorter side chains (13–17C) display increased anticancer activity, possibly caused by the high lipophilicity and membrane affinity. It should also be mentioned that the activity is heavily impacted by the alkyl resorcinol homolog composition.[45] Our compound, O4, is a 5-alkyl resorcinol with a 13C side chain that exhibited potent anticancer activity, thereby confirming the available literature. Finally, the structure-activity relationship of isocoumarins in anticancer has not been thoroughly studied. Yet, a study on human cervical cancer cells, HeLa, revealed that the C-3 side chain length could influence the cytotoxicity. The same study showed that C8-OCH_3 did not alter the activity.[46] Since O1 had a weak IC_{50} in our study, we cannot properly analyze the structural modifications affecting the cytotoxic activity, especially against our studied cell lines, H460 and HT-29. However, it appears that the type

of substitution at C-3 significantly affects cytotoxicity, and the long aliphatic chains could diminish the activity.

Conclusion

This is the first phytochemical investigation of Lebanese *O. natrix* in which five compounds were isolated and tested for their anticancer activity. Interestingly, compounds O3 and O4 have not been reported before in Ononis species, with O4 being rare. Anticancer testing revealed that compounds O4 and O5 showed significant inhibitory activities against colon cancer cells HT-29 and lung cancer cells H460. Additionally, all the tested compounds and CE showed either synergistic or additive effects when used in combination with the anticancer drug, sorafenib. The inhibitory effect of the standard sorafenib dose was achievable with lower concentrations when combined with the CE or the pure compounds. On the other hand, the combination of CE or any of its pure compounds with the standard dose of sorafenib resulted in potentiation of its inhibitory effect. These findings highlight initial evidence that *O. natrix's* CE or any of its pure compounds may serve as potential combination strategies in vitro, especially compounds O4 and O5. However, the present study is limited to preliminary analysis only, and extensive studies are needed to draw a conclusion regarding therapeutic efficacy. Further investigations should be conducted to elicit the specific mechanisms of action behind these compounds, their full safety, and efficacy profiles.

Acknowledgement

The authors would like to thank Dr. Mohamad Hamwi (Beirut Arab University, Beirut, Lebanon) for collecting the plant material that was used in this study.

Authors' Contribution

All authors made substantial contributions to conception and design, acquisition of data, or analysis and interpretation of data; took part in drafting the article or revising it critically for important intellectual content; agreed to submit to the current journal; gave final approval of the version to be published; and agreed to be accountable for all aspects of the work. All the authors are eligible to be authors as per the International Committee of Medical Journal Editors (ICMJE) requirements/guidelines.

Consent to Participate

Not applicable.

Consent for Publication

Not applicable.

Data Availability Statement

The original contributions presented in this study are included in the article/supplementary material. Further inquiries can be directed at the corresponding author(s).

Declaration of Conflicting Interests

The authors declared no potential conflicts of interest with respect to the research, authorship, and/or publication of this article.

Ethical Approval

This study does not involve experiments on animals or human subjects.

Funding

The authors received no financial support for the research, authorship, and/or publication of this article.

Informed Consent

Not applicable.

Use of Artificial Intelligence-assisted Tools

During the preparation of this manuscript/study, the authors did not use GenAI for any purposes, such as generating text, data, or graphics, or for study design, data collection, analysis, or interpretation of data. The authors have reviewed and edited the output and take full responsibility for the content of this publication.

Supplemental Material

Supplemental material for this article is available online.

ORCID iDs

Aya Chouman https://orcid.org/0009-0003-2368-250X
Maha Aboul Ela https://orcid.org/0000-0002-9411-4900
Kamal Bouhadir https://orcid.org/0000-0002-6375-1763
Bilal Azakir https://orcid.org/0000-0003-3084-0265
Abdalla El-Lakany https://orcid.org/0000-0003-2122-2289
Mohamad Ali M. Hijazi https://orcid.org/0000-0002-9829-235X

References

1. Singh N, Vayer P, Tanwar S, et al. Drug discovery and development: Introduction to the general public and patient groups. *Front Drug Discov* 2023; 3: 1201419. DOI: 10.3389/FDDSV.2023.1201419.
2. Sun D, Gao W, Hu H, et al. Why 90% of clinical drug development fails and how to improve it? *Acta Pharm Sin B* 2022; 12(7): 3049–3062. DOI: 10.1016/J.APSB.2022.02.002.
3. GBD 2023 Cancer Collaborators. The global, regional and national burden of cancer, 1990–2023, with forecasts to 2050: A systematic analysis for the Global Burden of Disease Study 2023. *Lancet* 2025; 406: 1565–1586. Doi: 10.1016/S0140-6736(25)01635-6
4. Smolarz B, Łukasiewicz H, Samulak D, et al. Lung cancer—epidemiology, pathogenesis, treatment and molecular aspect (review of literature). *Int J Mol Sci* 2025; 26(5): 2049. DOI: 10.3390/IJMS26052049.
5. Sung H, Ferlay J, Siegel RL, et al. Global cancer statistics 2020: GLOBOCAN estimates of incidence and mortality worldwide for 36 cancers in 185 countries. *CA Cancer J Clin* 2021; 71(3): 209–249.

6. Alqosaibi AI. Nanocarriers for anticancer drugs: Challenges and perspectives. *Saudi J Biol Sci* 2022; 29(6): 103298. DOI: 10.1016/J.SJBS.2022.103298.
7. Khan SU, Fatima K, Aisha S, et al. Unveiling the mechanisms and challenges of cancer drug resistance. *Cell Commun Signal* 2024; 22(1): 109. DOI: 10.1186/S12964-023-01302-1.
8. Sohi GK, Levy J, Delibasic V, et al. The cost of chemotherapy administration: A systematic review and meta-analysis. *Eur J Health Econ* 2021; 22(4): 605–620. DOI: 10.1007/S10198-021-01278-0.
9. Khan T, Ali M, Khan A, et al. Anticancer plants: A review of the active phytochemicals, applications in animal models, and regulatory aspects. *Biomolecules* 2019; 10(1): 47. DOI: 10.3390/BIOM10010047.
10. Chaachouay N and Zidane L. Plant-derived natural products: A source for drug discovery and development. *Drugs Drug Candidates* 2024; 3(1): 184–207. DOI: 10.3390/DDC3010011.
11. Li Z, Chen K, Rose P, et al. Natural products in drug discovery and development: Synthesis and medicinal perspective of leonurine. *Front Chem* 2022; 10: 1036329. DOI: 10.3389/FCHEM.2022.1036329.
12. Chouman A, El-Lakany A, Aboul-Ela M, et al. Review on phenolic constituents and pharmacological activities of genus Ononis. *J Appl Pharm Sci* 2025; 15(7): 027–036. DOI: 10.7324/JAPS.2025.234398.
13. Tohme G and Tohme H. *Illustrated flora of Lebanon.* 1st ed. Beirut, Lebanon: National Council for Scientific Research, 2007.
14. Mhamdi B, Abbassi F and Abdelly C. Chemical composition, antioxidant and antimicrobial activities of the edible medicinal *Ononis natrix* growing wild in Tunisia. *Nat Prod Res* 2015; 29(12): 1157–1160. DOI: 10.1080/14786419.2014.981188.
15. Öz BE, İşcan GS, Akkol EK, et al. Wound healing and anti-inflammatory activity of some Ononis taxons. *Biomed Pharmacother* 2017; 91: 1096–1105. DOI: 10.1016/J.BIOPHA.2017.05.040.
16. Cañedo LM, del Corral JM and San Feliciano A. 5-Alkylresorcinols from *Ononis natrix*. *Phytochemistry* 1997; 44(8): 1559–1563. DOI: 10.1016/S0031-9422(96)00755-8.
17. San Feliciano A, del Corral JM, Cañedo LM, et al. 3,4-Dihydroisocoumarins from *Ononis natrix*. *Phytochemistry* 1990; 29(3): 945–948. DOI: 10.1016/0031-9422(90)80052-I.
18. Yerlikaya S, Zengin G, Mollica A, et al. A multidirectional perspective for novel functional products: In vitro pharmacological activities and in silico studies on *Ononis natrix* subsp. hispanica. *Front Pharmacol* 2017; 8: 600. DOI: 10.3389/fphar.2017.00600.
19. Barrero AF, Sánchez JF and Rodríguez I. N-Δ13-docosenoylanthranilic acid and alkylresorcinols from *Ononis natrix* subsp. hispanica. *Phytochemistry* 1990; 29(6): 1967–1969. DOI: 10.1016/0031-9422(90)85049-L.
20. Bakrim S, El Omari N, El Hachlafi N, et al. Dietary phenolic compounds as anticancer natural drugs: Recent update on molecular mechanisms and clinical trials. *Foods* 2022; 11(21): 3323. DOI: 10.3390/FOODS11213323.
21. Jin ZJ. About the evaluation of drug combination. *Acta Pharmacol Sin* 2004; 25(2): 146–147.
22. Cao SS and Zhen YS. Potentiation of antimetabolite antitumor activity in vivo by dipyridamole and amphotericin B. *Cancer Chemother Pharmacol* 1989; 24(3): 181–186. DOI: 10.1007/BF00300240.
23. Fontana G, Bruno M, Sottile F, et al. The chemistry and the anti-inflammatory activity of polymethoxyflavonoids from Citrus genus. *Antioxidants (Basel)* 2022; 12(1): 23. DOI: 10.3390/antiox12010023.
24. Han S, Kim HM, Lee JM, et al. Isolation and identification of polymethoxyflavones from the hybrid Citrus, hallabong. *J Agric Food Chem* 2010; 58(17): 9488–9491. DOI: 10.1021/jf102730b.
25. Hase T, Ohtani K, Kasai R, et al. Revised structure for hortensin, a flavonoid from Millingtonia hortensis. *Phytochemistry* 1995; 40(1): 287–290.
26. San Feliciano A, Barrero AF, Medarde M, et al. An isocoumarin and other phenolic components of *Ononis natrix*. *Phytochemistry* 1983; 22(9): 2031–2033. DOI: 10.1016/0031-9422(83)80038-7.
27. Kozaki KI, Miyaishi O, Tsukamoto T, et al. Establishment and characterization of a human lung cancer cell line NCI-H460-LNM35 with consistent lymphogenous metastasis via both subcutaneous and orthotopic propagation. *Cancer Res* 2000; 60(9): 2535–2540.
28. Keller F, Bruch R, Schneider R, Meier-Hubberten J, Hafner M, Rudolf R. A scaffold-free 3-D co-culture mimics the major features of the reverse Warburg effect in vitro. *Cells*. 2020; 9(8): 1900.
29. Youssef AMM, Maaty DAM and Al-Saraireh YM. Qualitative chemical compounds analysis and in vitro estimation of anti-proliferative, antidiabetic and anti-Alzheimer's disease effects of *Ononis natrix* (L.) family Fabaceae. *Pharmacia* 2024; 71(1): 1–11. DOI: 10.3897/pharmacia.71.e119755.
30. Aksit H, Ozan E and Erenler R. Isolation, characterization, and antiproliferative activity of polymethoxyflavones from Mentha dumetorum. *Nat Prod J* 2023; 13(7): 20–26. DOI: 10.2174/2210315136662211251429 44.
31. Maurya P, Singh S, Gupta MM, et al. Characterization of bioactive constituents from the gum resin of Gardenia lucida and its pharmacological potential. *Biomed Pharmacother* 2017; 85: 444–456. DOI: 10.1016/J.BIOPHA.2016.11.049.
32. Hendrixson M, Gladkiy Y, Thyagarajan A, et al. Efficacy of sorafenib-based therapies for non-small cell lung cancer. *Med Sci (Basel)* 2024; 12(2): 20. DOI: 10.3390/MEDSCI12020020.

33. U.S. Food and Drug Administration, Center for Drug Evaluation and Research. NEXAVAR (sorafenib) label, https://www.fda.gov/medwatch (2025, accessed 23 February 2025).
34. Cabrera J, Saavedra E, Del Rosario H, et al. Gardenin B-induced cell death in human leukemia cells involves multiple caspases but is independent of the generation of reactive oxygen species. *Chem Biol Interact* 2016; 256: 220–227. DOI: 10.1016/J.CBI.2016.07.016.
35. Chen PY, Wang CY, Tsao EC, et al. 5-Demethylnobiletin inhibits cell proliferation, downregulates ID1 expression, modulates the NF-κB/TNF-α pathway and exerts antileukemic effects in AML cells. *Int J Mol Sci* 2022; 23(13): 7392. DOI: 10.3390/ijms23137392.
36. Tan KT, Li S, Li YR, et al. Synergistic anticancer effect of a combination of paclitaxel and 5-demethylnobiletin against lung cancer cell line in vitro and in vivo. *Appl Biochem Biotechnol* 2019; 187(4): 1328–1343. DOI: 10.1007/s12010-018-2869-1.
37. Goh JX, Tan LT, Goh JK, et al. Nobiletin and derivatives: Functional compounds from citrus fruit peel for colon cancer chemoprevention. *Cancers (Basel)* 2019; 11(6): 867. DOI: 10.3390/CANCERS11060867.
38. Rosas-Martínez M and Gutiérrez-Venegas G. Comparison of nobiletin and 5-demethylnobiletin as cancer chemopreventive agents. *Eur J Cancer Care (Engl)* 2024; 2024(1): 1128095. DOI: 10.1155/ECC/1128095.
39. Liu S, Zhang J, Yang H, et al. Pectolinarigenin flavonoid exhibits selective anti-proliferative activity in cisplatin-resistant hepatocellular carcinoma, autophagy activation, inhibiting cell migration and invasion, G2/M phase cell cycle arrest and targeting ERK1/2 MAP kinases. *J BUON* 2020; 25(1): 415–420.
40. Deng Z, Shen D, Yu M, et al. Pectolinarigenin inhibits bladder urothelial carcinoma cell proliferation by regulating DNA damage/autophagy pathways. *Cell Death Discov* 2023; 9(1): 214. DOI: 10.1038/s41420-023-01508-9.
41. Lu M, Kong Q, Xu X, Lu H, Lu Z, Yu W, et al. Pectolinarigenin-A flavonoid compound from Cirsium Japonicum with potential anti-proliferation activity in MCF-7 breast cancer cell. *Trop J Pharm Res* 2014; 13(2): 225–8. DOI: 10.4314/tjpr.v13i2.9
42. Abdu S, Juaid N, Amin A, et al. Effects of sorafenib and quercetin alone or in combination in treating hepatocellular carcinoma: In vitro and in vivo approaches. *Molecules* 2022; 27(22): 8082. DOI: 10.3390/MOLECULES27228082.
43. Li J, Zhang L, Ge T, et al. Understanding sorafenib-induced cardiovascular toxicity: Mechanisms and treatment implications. *Drug Des Devel Ther* 2024; 18: 829–843. DOI: 10.2147/DDDT.S443107.
44. Aidiel M, Abdul Mutalib M, Ramasamy R, et al. Mechanistic insights into the anticancer potential of methoxyflavones analogs: A review. *Molecules* 2025; 30(2): 346. DOI: 10.3390/MOLECULES30020346.
45. Marentes-Culma R and Coy-Barrera E. Comparative evaluation of 5-n-alkylresorcinol extraction conditions from wheat bran via metabolite profiling: Implications for antiproliferative activity. *Foods* 2025; 14(12): 2108. DOI: 10.3390/FOODS14122108.
46. Guo Z, Chen B, Chen D, et al. New isocoumarin and pyrone derivatives from the Chinese mangrove plant Rhizophora mangle-associated fungus Phomopsis sp. DHS-11. *Molecules* 2023; 28(9): 3756. DOI: 10.3390/MOLECULES28093756.

Abbreviations

^{13}C-NMR: Carbon-13 NMR
^{1}H-NMR: Proton NMR
CC: Column chromatography
$CDCl_3$: Deuterated chloroform
CD_3OD: Deuterated methanol
Conc. NH_3: Concentrated ammonia
COSY: Homonuclear correlation spectroscopy
DCM: Dichloromethane
DEPT: Distortionless enhancement by polarization transfer
DMSO: Dimethyl sulfoxide
DMSO-d_6: Deuterated dimethyl sulfoxide
EtOAc: Ethyl acetate
FT-IR: Fourier transform infrared spectroscopy
H460: Human non-small cell lung cancer cell line
HMBC: Heteronuclear multiple bond correlation
HSQC: Heteronuclear single quantum coherence
HT-29: Human colon adenocarcinoma cell line
IC_{50}: Half-maximal inhibitory concentration
MeOH: Methanol
MF: Molecular formula
MHz: Megahertz
MW: Molecular weight
NMR: Nuclear magnetic resonance
NOESY: Nuclear Overhauser effect spectroscopy
PE: Petroleum ether
TLC: Thin-layer chromatography